

Review

Theory-Guided Design of Organic Electro-Optic Materials and Devices

Larry Dalton * and Stephanie Benight

Departments of Chemistry & Electrical Engineering, University of Washington, Seattle, WA 98195, USA; E-Mail: sbenight@uw.edu

* Author to whom correspondence should be addressed; E-Mail: dalton@chem.washington.edu; Tel.: +1-360-981-4575; Fax: +1-206-685-8665.

Received: 15 July 2011; in revised form: 2 August 2011 / Accepted: 16 August 2011 /

Published: 19 August 2011

Abstract: Integrated (multi-scale) quantum and statistical mechanical theoretical methods have guided the nano-engineering of controlled intermolecular electrostatic interactions for the dramatic improvement of acentric order and thus electro-optic activity of melt-processable organic polymer and dendrimer electro-optic materials. New measurement techniques have permitted quantitative determination of the molecular order parameters, lattice dimensionality, and nanoscale viscoelasticity properties of these new soft matter materials and have facilitated comparison of theoretically-predicted structures and thermodynamic properties with experimentally-defined structures and properties. New processing protocols have permitted further enhancement of material properties and have facilitated the fabrication of complex device structures. The integration of organic electro-optic materials into silicon photonic, plasmonic, and metamaterial device architectures has led to impressive new performance metrics for a variety of technological applications.

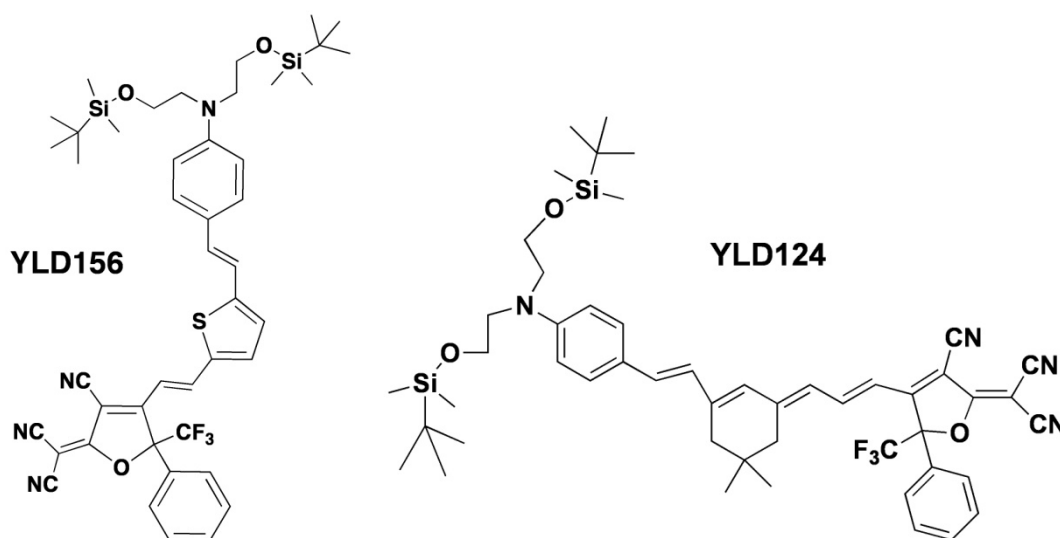
Keywords: organic electro-optic materials and devices; electric field poling; chromophores with high molecular first hyperpolarizability; laser-assisted poling; time-dependent density functional theory; course-grained Monte Carlo and molecular dynamics methods; nano-engineering of intermolecular interactions; silicon photonics; plasmonics; metamaterials

1. Introduction

A number of factors have motivated interest in organic electro-optic (OEO) materials over the past two-plus decades. The ubiquitous femtosecond phase relaxation times of π -electron chromophores raise the possibility of terahertz bandwidth in device applications [1-4]. This potential has been demonstrated in all-optical switching and optical rectification [1,2], terahertz generation and detection [3], and in femtosecond pulse experiments [4]. However, more frequently, device bandwidth will be defined by the properties of other materials such as the resistivity of electrode materials (e.g., metals or doped silicon) used in devices such as Mach Zehnder modulators [5,6]. Electrode resistivity commonly limits device bandwidths to 100 GHz or less. Thus, optimization of device bandwidth has largely been an issue of device design (electrode engineering) with shorter electrical/optical interactions lengths leading to higher bandwidth. If a material with large electro-optic activity can be utilized in device fabrication, a shorter device length can still be employed for realization of high bandwidth without device drive voltages becoming excessively high. In other words, drive voltages and bandwidth are related and can be traded off.

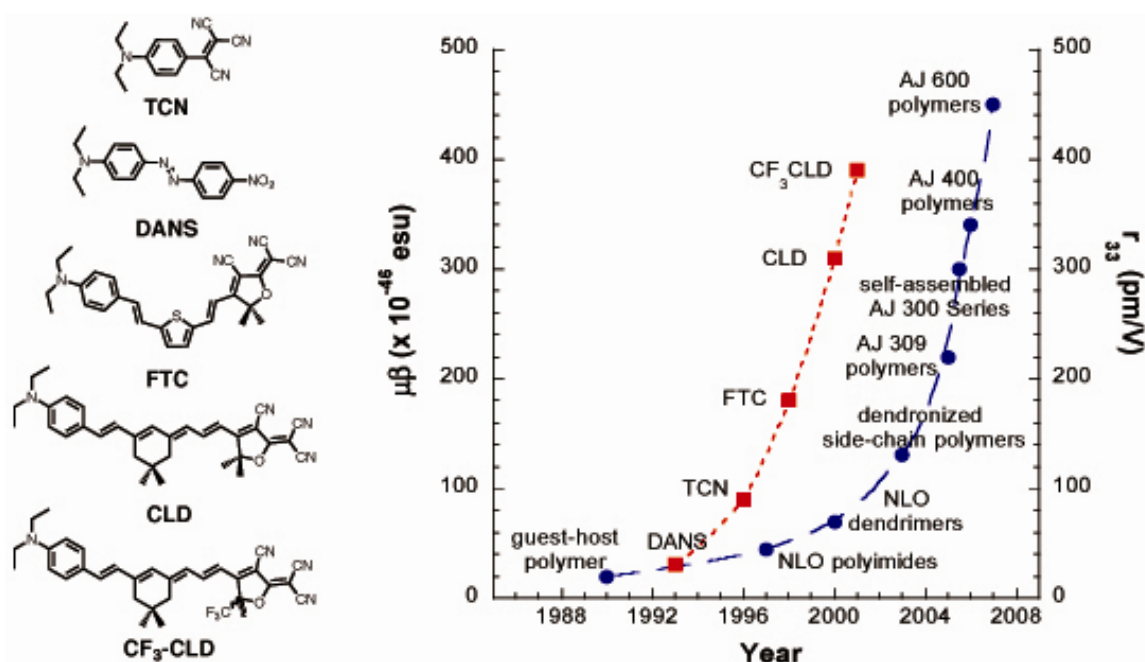
A second factor, which has motivated interest in OEO materials, is the potential for exceptional electro-optic activity, *i.e.*, large electro-optic coefficients. In the late 1980s and 1990s, belief in this potential was a major driving force for synthesizing new materials although during that period electro-optic activity of OEO materials essentially remained less than that of lithium niobate (*i.e.*, below 30–32 pm/V). There are two reasons for early failure to realize large electro-optic activity: (1) Difficulties in producing chromophores with large molecular first hyperpolarizability which also exhibited prerequisite thermal, chemical, and photochemical stability and (2) difficulties associated with translating large molecular optical nonlinearity into large macroscopic (bulk) material optical nonlinearity (electro-optic activity). A major advance in overcoming the first road block was achieved in the late 1990s with introduction of chromophores based on the tricyanovinylfuran (TCF) acceptor moiety (see Figure 1) [7]. As illustrated in Figure 1, OEO chromophores are charge-transfer (dipolar) molecules that can be described as constituted from donor, bridge, and acceptor modules [7].

Figure 1. The YLD156 chromophore, utilizing a heteroaromatic bridge, is shown on the left and the YLD124 chromophore, utilizing on a polyene bridge, is shown on the right.



Throughout the history of OEO research, the donor moiety has largely been of the amine structure shown. Bridge moieties have consisted of heteroaromatic or polyene structures including isophorone-protected polyene structures (see Figure 1). Early OEO materials contained acceptor moieties based on nitro, cyano, alkoxy, isoxazolone, tricyanovinyl, 1,3-bis(dicyanomethylidene)indane, and diarylthiobarbituric acid groups [7]. Introduction of the TCF acceptor led to significant increase in molecular first hyperpolarizabilities (β) and exceptional stability [7] as is illustrated in Figure 2 [8].

Figure 2. The chronological variation of the product of chromophore first hyperpolarizability (β) and dipole moment (μ) is shown in red (dotted line) while the variation of electro-optic activity (r_{33}) is shown in blue (dashed line). Adapted from reference [8] with permission of the American Chemical Society.



The efficient translation of large molecular nonlinearity into large macroscopic nonlinearity has proven to be more elusive. Noncentrosymmetric (or acentric) order is required for non-zero macroscopic electro-optic activity. Indeed, electro-optic activity is proportional to the product of chromophore number density (N , molecules/cc), molecular first hyperpolarizability (β), and the acentric order parameter ($\langle \cos^3\theta \rangle$). A severe problem observed for early chromophore-polymer composite OEO materials prepared by electric field poling was that electro-optic activity went through a maximum as a function of chromophore number density and this maximum shifted to lower number density with increasing chromophore dipole moment (μ) and molecular first hyperpolarizability (β) [7]. This is because chromophore-chromophore dipolar interactions tend to drive centric pairing of chromophores at high concentrations. Throughout the 1990s chromophore loading in polymers was limited to about 20% and acentric order parameters to about 0.1 with the net result that only about 2% of the potential EO activity of chromophores was being translated to macroscopic (material) EO activity. In the late 1990s, an important theoretical advance was achieved by noting that there are two components of the chromophore-chromophore dipolar interaction potential with one favoring centric order and the other favoring acentric order [9-11]. The relative importance of these two components

could be shifted by control of chromophore shape. Thus, shape engineering became an important pursuit in optimizing the performance of chromophore-polymer composite materials [12]. Correlated quantum/statistical mechanical investigation of structure/function relationships is relevant to such shape engineering and permitted development of OEO materials that, for the first time, exceeded the electro-optic activity of lithium niobate. Such electro-optic activity was still below the non-interacting particle limit for a three-dimensional (Langevin) lattice (*i.e.*, for non-interacting particles, $\langle \cos^3\theta \rangle \sim \mu E_{\text{pol}}/5kT$ or about 0.2 for a normalized poling energy, $\mu E_{\text{pol}}/kT$, of unity). Simple theoretical calculations suggest, that for a given normalized poling energy, acentric order (and thus electro-optic activity) can be increased by reducing lattice dimensionality experienced by the OEO chromophore [13,14]. For example for non-interacting particles and unity normalized energy, $\langle \cos^3\theta \rangle \sim \mu E_{\text{pol}}/3kT$ for a 2-D (Bessel) lattice and $\langle \cos^3\theta \rangle \sim 3\mu E_{\text{pol}}/4kT$ for a 1-D (Ising) lattice. Since 2005, efforts to improve EO activity have largely focused on the theory-inspired, systematic control of intermolecular electrostatic interactions and lattice dimensionality. This work will be a major focus in the next section.

However, a large electro-optic activity is a necessary but not sufficient requirement for a practical advance in OEO device technology. Thermal and photochemical stability are also required. Electric field poling-induced acentric order and accompanying electro-optic activity are not thermodynamically stable. The rate at which poling-induced order is lost is related to the difference between the material glass transition temperature (T_g) and the measurement (or device operational) temperature [7,15,16]. The T_g needs to be at least 50 °C above the operational temperature to achieve stability that will satisfy Telcordia standards. For chromophore-polymer composite materials, this required using host polymer materials (such as polyimides or polycarbonates) with glass transition temperatures above 150 °C. Such high glass transition temperatures in turn require high poling temperatures, which can result in sublimation of chromophores and other unwanted effects [7,15,16]. An alternative to a final high glass transition OEO material involves crosslinking subsequent to introduction of acentric order by electric field poling [7,15,16]. Initial research into lattice hardening by crosslinking involved exploitation of free radical and condensation reactions [7]. More recently, these protocols have been replaced by lattice hardening based on utilization of cycloaddition reactions including those involving the fluorovinyl ether moiety [16-18] and Diels-Alder/Retro-Diels-Alder reactions [16,19-21]. The latter class of reactions has been particularly successful in yielding final material glass transition temperatures as high as 300 °C [16,19-21]. Cycloaddition reactions involve minimal lattice disruption in contrast to earlier methods, *e.g.*, lattice disruption associated with evolution of condensation products [7,22]. Electro-optic devices manufactured by Lumera/Gigoptix have met Telcordia standards.

Photochemical stability is essentially defined by the production and reaction of singlet oxygen [16]. The hardness of the lattice dramatically influences the rate of degradation as does packaging of OEO materials and devices. Steric protection of reactive positions within the OEO chromophore and the addition of quenchers of singlet oxygen also have major effects. Current materials routinely yield results under accelerated testing that suggest stability of greater than ten years at traditional telecommunication power levels.

Optical loss is also an important consideration. Indeed, a figure-of-merit (FOM) that has been suggested for electro-optic materials is electro-optical activity (*e.g.*, an operationally utilized element of the electro-optic tensor such as r_{33}) divided the response time (τ) and the total material optical loss

(MOL). There are three elements of total device-relevant optical loss: (1) absorption loss associated with either electronic or vibrational transitions; (2) processing-induced loss associated with introduction light scattering; and (3) coupling losses associated with either index of refraction or mode size mismatch in terms of getting light into and out of device structures. With OEO materials minimization of optical loss from interband (charge transfer) electronic absorption requires operating at wavelengths sufficiently far removed from the electronic absorption band and avoiding the introduction of excitonic contributions from chromophore aggregation during material processing. Minimization of vibrational absorption loss requires control of hydrogen concentration in OEO materials. This is usually achieved by utilization of dendritic structures and/or partial fluorination of OEO materials. With these two absorption minimization protocols effectively implemented, total absorption loss can be reduced to approximately 0.2 dB/cm, which is very comparable to the loss observed for lithium niobate. However, values of 1–2 dB/cm are more common for OEO materials. Scattering loss observed in OEO waveguides arises from a variety of contributions including phase-separation induced in spin casting or poling of materials, material damage associated with electric field poling, and scattering losses arising during the fabrication of waveguide structures (associated with waveguide wall roughness). With care, scattering losses can be kept to insignificant values although integration of OEO materials into nanoscopic silicon photonic waveguide structures frequently involves dealing with optical losses associated with the roughness of silicon waveguides on the order of 2 dB/cm. Coupling losses can easily be the dominant source of total insertion loss; however, the use of special coupling structures can reduce coupling losses to very acceptable values, e.g., total insertion loss (material, processing, and coupling) values of 6 dB or less [23-29].

A relatively unappreciated advantage of OEO materials is the fact that these materials can be tailored to be compatible with a wide variety of materials (e.g., metals, metal oxides, *etc.*) and processing options (e.g., vapor and solution deposition, nanoimprint lithography, lift-off techniques, *etc.*). For example, soft and nanoimprint lithography techniques permit rapid and cost effective production of complex photonic circuitry such as coupled ring resonators [30]. Lift-off techniques permit fabrication of conformal and flexible devices [31]. Three-dimensional (3-D) optical circuitry has been fabricated using a variety of masking techniques including grayscale lithography [32].

A recently demonstrated advantage of OEO materials is the ease of integration into silicon photonic, plasmonic, and metamaterial device structures [1,2,33-51]. Concentration of optical and electric fields in such devices facilitates the more effective utilization of the large electro-optic coefficients and material bandwidth (fast switching speeds) characteristics of OEO materials. Demonstration of sub-1 volt GHz operational voltages has become common and operational voltages as low as 10 millivolts are not out of the question as loss and bandwidth issues in the fabrication of silicon (and silicon nitride) photonics, plasmonics, and metamaterial architectures are more effectively addressed. Material conductivity has become an issue in the engineering of more complex materials and devices, particularly as it affects poling efficiency in the introduction of OEO material electro-optic activity in specific device structures. Conductivity problems have motivated interface engineering efforts such as the introduction of nanoscopic metal oxide (e.g., titanium dioxide) between drive electrodes and OEO materials [16,52]. Such charge blocking layers inhibit injection and withdrawal of charge to and from OEO materials associated with control of material (electrode metal or metal oxide and electro-optic material) work functions and inhibiting quantum mechanical tunneling of charge across interfaces.

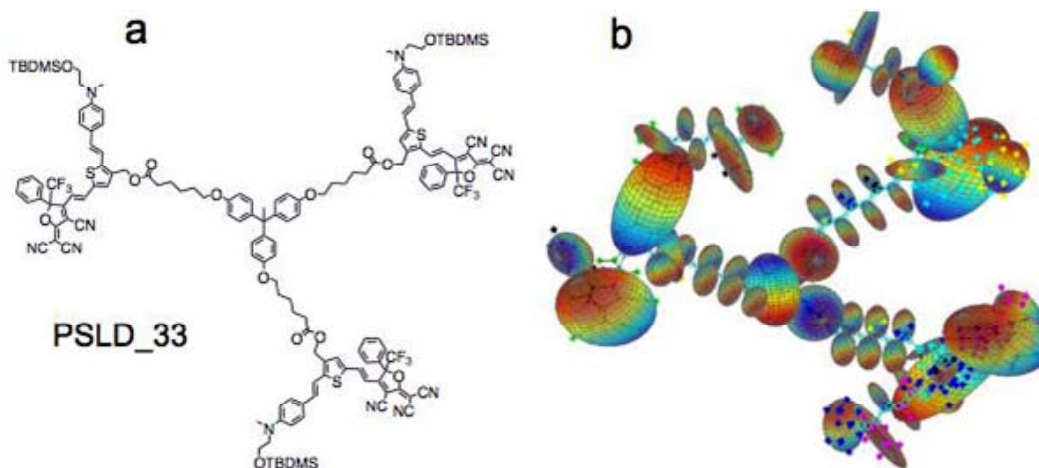
Another route to dealing with OEO material conductivity at poling temperatures is to employ lower poling voltages but this involves utilizing materials with exceptional poling efficiencies. This brings us to the topic of the next section; namely, the engineering of intermolecular electrostatic interactions in materials so that such interactions dramatically enhance poling efficiency. As noted above, one route to enhancement of poling efficiency is the reduction in lattice dimensionality that the OEO chromophore experiences.

2. Materials Development

A starting point for the development of new materials is definition of material structure-function relationships to guide that development. Quantum and statistical mechanics have played a critical role in the engineering of simple molecular materials; however, the complexity of OEO materials poses a challenge for use of such methods. Recently, the utility of computation of linear and nonlinear optical properties of OEO materials including the dependence of properties on dielectric permittivity [53,54] and optical frequency [55-57] by time-dependent density functional theory, TD-DFT (including real-time time-dependent density functional theory, RT-TD-DFT [55-57]) has been advanced. Improvements have been based on careful correlation of theoretical and experimental data and on the development of new hybrid functionals (e.g., M06-2X gives better reproduction of trends in OEO materials going from heteroaromatic bridges, e.g., YLD156, to polyene bridges, e.g., YLD124, compared to the highly utilized B3LYP functional). However, it should be noted that B3LYP has provided good quantitative simulation of molecular hyperpolarizabilities for a range of materials.

Fully atomistic Monte Carlo (MC) and molecular dynamics (MD) statistical mechanical methods [58-61] are useful for simulation of material properties but are too demanding of computational resources and time to be of general utility. Course graining of such methods, as illustrated in Figure 3, has permitted extension of these methods to complex polymer and dendrimer OEO materials [62-65].

Figure 3. Chemical and Pseudo-Atomistic structures for an EO dendrimer are shown. Reproduced from reference [65] with permission of the American Chemical Society.

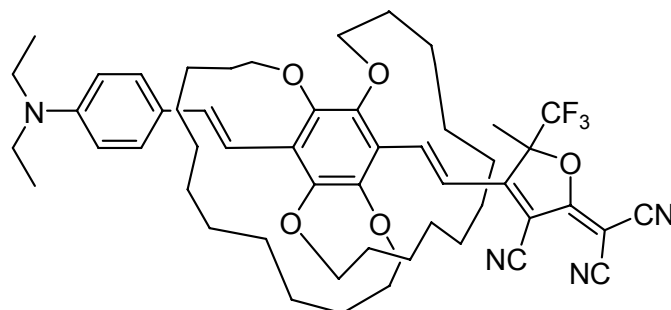


Course-grained or pseudo-atomistic MC/MD methods are useful for OEO materials as extended π -electron conjugation inhibits rotation about π -bonds. Thus, application of a “United Atom”

approximation to phenyl groups and OEO chromophores is sensible and has been demonstrated to be as accurate as fully-atomistic calculations. The coupling of these “new” quantum (new hybrid functional TD-DFT and RT-TD-DFT) and statistical (PAMC/MD) mechanical methods has permitted development of reliable structure-function relationships for all classes of OEO materials. Let us now review these different classes of materials and the relationships critical for the optimization of each class of material.

The first and most simple class of OEO materials to be considered is chromophore-polymer composite materials prepared by dissolving OEO chromophores in a non-NLO active (typically, commercially available) polymer host such as polymethylmethacrylate (PMMA), polymer carbonate (PC), amorphous polycarbonate (APC), polyquinoline (PQ), or polyimide (PI). Both fully atomistic MC/MD and pseudo-atomistic PAMC/MD methods have shown that chromophore-host interactions can be neglected to good approximation and poling-induced order is dominated by the competition of chromophore dipole-electric poling field interactions with chromophore-chromophore dipolar interactions. Both analytical [9,10,62] and numerical [11,63-66] methods have demonstrated that there are two components to the chromophore-chromophore dipolar interaction potential. One component favors centrosymmetric (centric) chromophore organization while the other favors noncentrosymmetric (acentric) organization with the weighting of the contributions from these two components determined by chromophore shape (steric or nuclear repulsive potentials). Unfortunately, even the best chromophore shape (spherical) does not permit exceeding the Langevin limit for acentric order, *i.e.*, chromophores behave as if they exist in a 3-D lattice [63]. The variation of electro-optic activity (e.g., r_{33}) with chromophore number density (N) will always be less than the limit expected for non-interacting dipolar molecules (which is a linear dependence of r_{33} on N defined by the molecular first hyperpolarizability and the effective poling field experienced by the chromophores). However, there continues to be considerable research on modification of chromophore structure (as first demonstrated in [12]) to achieve improved EO activity. Such modification is now commonly referred to as “site isolation” and is an alternative to site isolation achieved by lowering chromophore concentration in composite materials [67-71]. An example of such modification of is shown in Figure 4 [71].

Figure 4. The CZC7a chromophore modified to approximate a spherical shape is shown.



For this material, the behavior of r_{33} vs. N is Langevin (in good agreement with theory) with the maximum in EO activity corresponding approximately to the neat material. Note that doping this material into APC is used to observe the full concentration range but no aggregation leading to phase separation is observed for the neat material. Although the neat material exhibits good processability and could be used for device fabrication, the phenyl ring of the chromophore interrupts π -conjugation

leading to low molecular first hyperpolarizability. Thus electro-optic activity (the maximum observed EO activity is approximately 23 pm/V) is too low for practical application despite the high number density and reasonable (Langevin limit) order parameter. For currently available core chromophore architectures, the maximum electro-optic activity achieved for chromophore-polymer composites is typically less than 120 pm/V (50–100 pm/V are the most commonly observed values).

The second and slightly more complex class of materials considered involves chromophores covalently incorporated into non-NLO active polymer and dendrimer matrices (e.g., such as shown in Figure 3). For such materials, the restrictions placed on chromophore organization by covalent bonds (covalent bond potentials) must be taken into account. In the PAMC/MD approach, atoms involved in sigma bonds are treated by fully atomistic methods and atoms involved in conjugated pi bond structures are treated within the United Atom Approximation. If segments connecting chromophores to the core polymer or dendrimer structure are very flexible, the poling-induced organization is essentially the same as found for the chromophore in a composite material, *i.e.*, one can neglect chromophore-host interactions). However, if covalent bond potentials prevent chromophores from pairing centrosymmetrically, then the behavior approaches that expected for independent particles, *i.e.*, a linear dependence of r_{33} on N . Such behavior is observed for the three-chromophore-containing dendrimer of Figure 3 and for related dendrimers [65,72]. An advantage of covalent incorporation of chromophores is that high chromophore number densities can be obtained without chromophore phase separation. For example, the OEO material (PSLD_33) shown in Figure 3, has a number density of $\sim 6.5 \times 10^{20}$ molecules/cc, *i.e.*, about three times the maximum loading achievable for the core (YLD156-type) chromophore in a chromophore-polymer composite. Decreasing the number density by creating higher generation versions of the PSLD_33 dendrimer results in an observed (and theoretically-predicted) linear variation of r_{33} with N as does decreasing number density by dissolving dendrimers in polymer hosts such as APC [65,72]. For such materials, the observed electro-optic activity is typically above 150 pm/V but less than 250 pm/V. Conductivity issues encountered at high concentrations act to attenuate realizable EO activity.

We now consider materials where intermolecular electrostatic interactions improve poling efficiency (*i.e.*, r_{33}/E_{pol} where E_{pol} is the poling field strength) leading to a linear variation of electro-optic activity with chromophore number density that exceeds the non-interacting particle limit. We refer to such materials as “matrix-assisted poling (or MAP)” materials and we will demonstrate that the improvement in poling efficiency can be viewed as resulting from a reduction in lattice dimensionality. We will introduce the concept of fractional lattice dimensionality (M) appropriate for non-perfectly-ordered (Boltzmann) materials and will show how such fractional lattice dimensionality (M) can be quantitatively defined experimentally. In the next section we will introduce experimental techniques for defining lattice dimensionality from the ratio of centric and acentric order parameters and for defining the structure and dynamics (e.g., nanoscale viscoelasticity) associated with reduced dimensionality and molecular cooperativity. Both nanostructural and thermodynamic characterizations of the role of specific spatially-anisotropic intermolecular interactions are presented.

MAP materials involve the introduction of molecular cooperativity associated with specific spatially-anisotropic intermolecular electrostatic interactions. Perhaps the simplest example is that of binary chromophore organic glasses (BCOGs) [8,64,73,74] which are composite materials where both guest and host are chromophore-containing materials, e.g., a chromophore guest dissolved in a

chromophore-containing polymer or dendrimer host. A practical example is the YLD124 chromophore (Figure 1) dissolved in the PSLD_33 dendrimer material (Figure 3). Guest and host chromophores can experience dipolar interactions and the poling field will affect both guest and host. The poling field will reduce the effective lattice dimensionality of both guest and host and the intermolecular electrostatic interaction between the two can further amplify the effect leading to enhanced poling efficiency through MAP. The effect on r_{33} or r_{33}/E_{pol} is to result in a new linear dependence with an enhanced slope. Of course, the shapes of guest and host chromophores can play an important role in defining the detailed assembly of the chromophores [64]. Very high chromophore concentrations can be achieved without phase separation for BCOGs because one is dissolving a polar guest into a polar host in contrast to traditional composite materials where a polar guest is being dissolved into a nonpolar host. As expected because the dielectric environment is not changing with relative concentrations of guest and host materials, solvatochromic shifts are not observed, in contrast to the observation of large shifts observed for conventional composite materials. The absence of solvatochromic shifts and phase separation frequently results in low optical absorption and scattering loss. Plasticization of the material glass transition observed for traditional composite materials typically does not occur with BCOGs. MAP intermolecular electrostatic interactions also generally lead to improve thermal and photochemical stability. The high chromophore number densities (e.g., $>5 \times 10^{20}$ molecules/cc) achieved with BCOGs contributes to improved macroscopic electro-optic activity but can also contribute to material conductivity at poling temperatures and to absorption loss unless care is exercised in design of chromophore structures and in design of poling configurations (*i.e.*, control of processing conditions). Obviously, the critical aspect of MAP materials is the control of intermolecular electrostatic interactions between guest and host chromophores by control of chromophore dipolar interactions and steric (nuclear repulsive) or shape interactions so that the reduction in lattice dimensionality effected by the chromophore-poling field interactions can be effectively exploited.

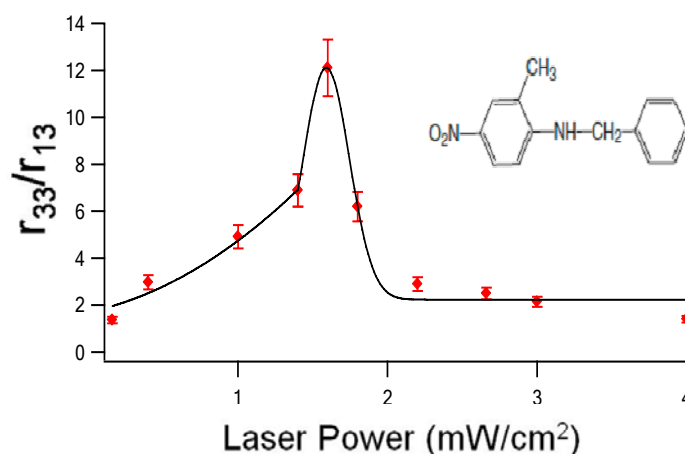
Laser-assisted electric field poling (LAEFP or LAP for short) [73-75] can also be used to reduce effective lattice dimensionality and improve electro-optic activity. An early demonstration of this effect involved incorporating a high $\mu\beta$ chromophore guest (e.g., YLD124 or YLD156) into a DR1-*co*-PMMA chromophore host (which is commercially available from Aldrich Chemical). The disperse red DR1 chromophore is known to undergo photo-induced (photochromic) trans-cis-trans isomerization with the net effect being photo-driven molecular reorientation. If polarized light is used, the DR1 chromophores can be driven into a 2-D lattice structure. If the guest chromophore interacts with the host chromophores, the guest experiences an effective 2-D lattice. Thus, the effective electro-optic activity of both guest and host is increased with the observed electro-optic activity being the sum of the two.

LAP can also be applied to a single pure chromophore material if intermolecular electrostatic interactions that drive acentric organization exist between chromophores. An example (see Figure 5) is provided by vapor deposited BNA (which forms acentric single crystals in melt or solution processing) [75].

In this case, LAP can be viewed as producing orientation-selective melting with the intermolecular electrostatic interactions among the BNA molecules driving crystal growth in the direction of the electric poling field. Because chromophores pointing in the direction of the poling field are not heated (the chromophore charge-transfer band transition moment is \sim zero for that orientation), the net effect is

the generation of acentric thin film order in a direction appropriate for device application. Acentric order parameters as high as 0.95 have been obtained but the graph of Figure 5 indicates how sensitive generation of optimum EO activity is to poling conditions. This approach produces desired correctly-oriented thin film materials much more rapidly and avoids the problems of orienting crystals with undesirable growth anisotropy obtained with traditional single crystal growth.

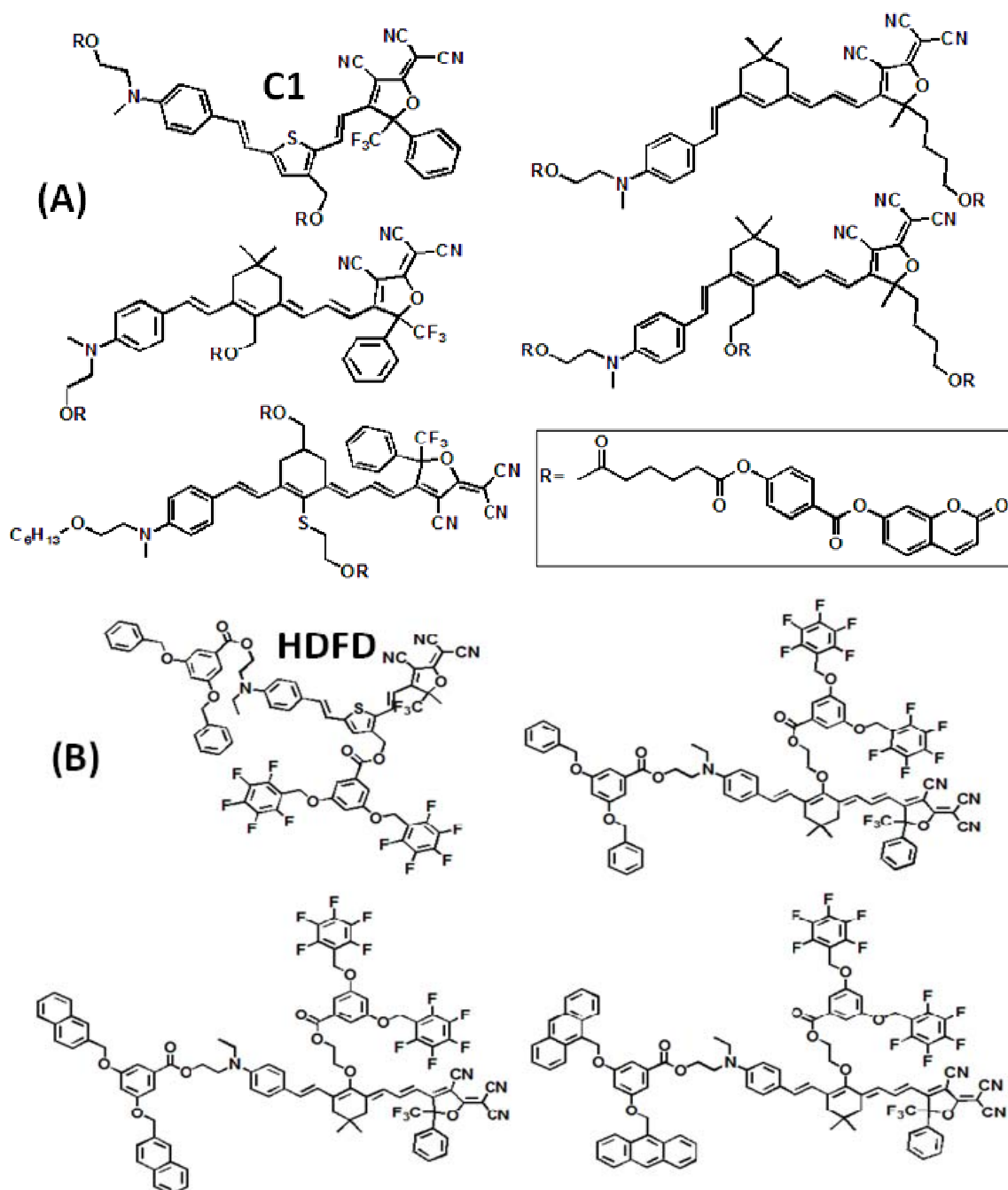
Figure 5. The structure of BNA is shown at the upper right (inset) and below the variation of the ratio r_{33}/r_{13} is shown as a function of laser power used in LAP. A value of the ratio near 3 indicates low order while increasing values of the ratio are consistent with a larger acentric order parameter and reduced dimensionality.



The preceding example of BNA involves strong intermolecular electrostatic interactions among small molecules with modest chromophore-chromophore dipolar interactions. The difficulty with strong interactions, including ionic and hydrogen bonding interactions which are important for the formation of many crystalline materials, is that these strong interactions can elevate material melting (or glass transition) temperatures above material decomposition temperatures. Most OEO materials start to exhibit decomposition above 300 °C. If decomposition occurs before melting, then melt processability is lost. A fruitful avenue for development of improved OEO materials would seem to be the exploration of a number of dipolar and quadrupolar interactions that can be introduced to achieve MAP but which do not inhibit melt processing. Here we discuss dipolar interactions based on the intermolecular electrostatic interactions of coumarin moieties (which are known to be critical in formation of certain liquid crystalline phases) and quadrupolar interactions operative in arene-perfluoroarene dendritic materials. Representative molecular structures are shown in Figure 6. Such interactions induce molecular cooperativity for the coumarin-containing or arene-perfluoroarene-containing dendrimers of Figure 6 that are on the order of 100 nm at the poling temperature. Such molecular cooperativity results in effective 2-D lattices and theoretically-predicted approximate factors of two enhancements of order parameters. Molecular cooperativity also affects nanoscale viscoelasticity and the thermodynamics (energetic) of various phases of matter including phases of reduced dimensionality. The viscoelastic properties can be characterized by nanoscopic measurement techniques such as shear modulation force microscopy (SM-FM) [76-79] and intrinsic friction analysis (IFA) [80]. They can also be studied by dielectric relaxation spectroscopy (DRS) [81,82] and by differential scanning calorimetry (DSC). As thermal transition is made between various phases of

matter, the corresponding viscoelastic properties change. A well-known transition in polymer and dendrimer materials is the material melting or glass transition temperature, T_g . If interactions that promote molecular cooperativity are present then a lower temperature transition is observed associated with changes in effective lattice dimensionality.

Figure 6. Dendritic structures based on exploiting dendron (or pendant) intermolecular interactions are shown. The prototypical coumarin dendrimer (A) and arene-perfluoroarene dendrimer (B) structures are denoted C1 and HDFD respectively.

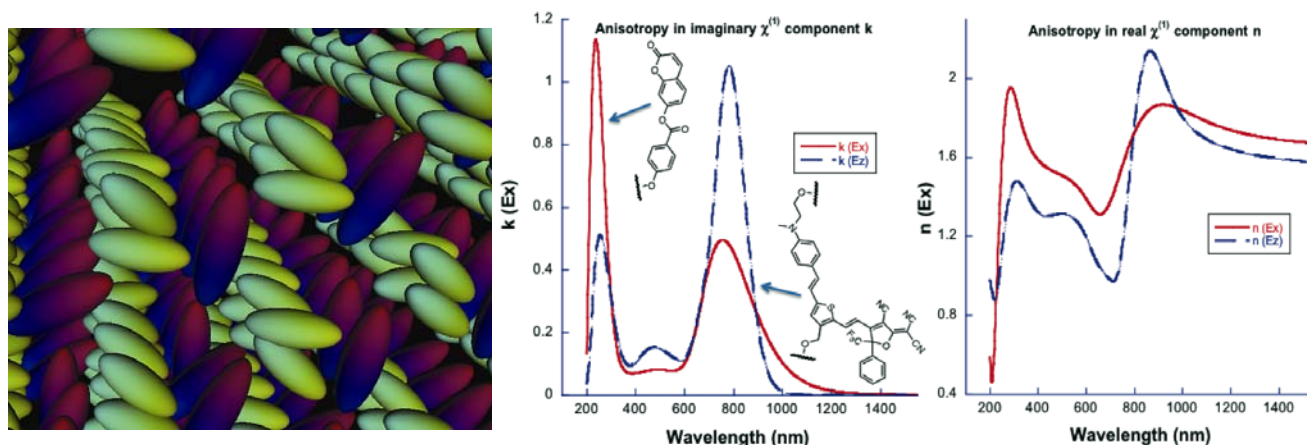


Molecular organization and lattice dimensionality can be defined by measurement of acentric ($\langle \cos^3 \theta \rangle$) and centric ($\langle \cos^2 \theta \rangle$ or $\langle P_2 \rangle$ where $2\langle P_2 \rangle = 3(\langle \cos^2 \theta \rangle - 1)$) parameters. Theory demonstrates that effective (including fractional) lattice dimensionality, M , can be defined by the

relationship between acentric and centric order parameters; namely, $[\langle \cos^3\theta \rangle]^2 = \{(9 - 2M)/(2 + M)\} \langle P_2 \rangle - \{(3 - M)/2M\}$. Experimentally, the acentric order parameter can be defined using techniques such as attenuated total reflection (ATR) [83-85], two-slit interferometry (TSI) [86,87], Fabry-Perot interferometry (FPI) [88], or a Mach Zehnder interferometric technique (MZI) [89], which permit measurement of both of the two non-zero electro-optic tensor elements, r_{33} and r_{13} , for poled OEO materials. The acentric order parameter can be extracted either from the ratio of r_{33}/r_{13} or from r_{33} alone if the elements of the molecular first hyperpolarizability tensor (e.g., β_{zzz}) are correctly estimated from a combination of quantum mechanical calculations and hyper-Rayleigh scattering (HRS) measurements [53,90,91] and/or electric field induced second harmonic generation (EFISH) measurements [16]. Figure 5 illustrates the variation of the ratio r_{33}/r_{13} with LAP optical power (orientation-selective heating) illustrating how these change with increasing order. The maximum in the plot in the ratio of r_{33}/r_{13} also corresponds to the maximum in the graph of r_{33} . The ratio of minor to major elements of the β tensor is estimated to be 1/6 for BNA from the data of Figure 5 and single crystal measurements. Quantum mechanical calculations of β are also consistent with this result.

The centric order parameter, $\langle \cos^2\theta \rangle$ or $\langle P_2 \rangle$, can be measured using variable angle polarization referenced absorption spectroscopy (VAPRAS) [92] or variable angle spectroscopic ellipsometry (VASE) [93,94]. VASE has the advantage of permitting simultaneous definition of $\langle P_2 \rangle$ order for both chromophore and dendrimer pendant, e.g., for the C1 chromophore of Figure 6, $\langle P_2 \rangle \sim +0.2$ while the $\langle P_2 \rangle$ for the coumarin moiety is ~ -0.2 . The VASE data (see Figure 7) clearly indicates that the chromophores and pendant lie in orthogonal planes. For the C1 chromophore, $\langle \cos^3\theta \rangle = 0.15$ (from ATR and HRS data together with quantum mechanical calculations). The ratio of acentric to centric order parameters suggest that the material lattices observed for the coumarin (C1) and arene-perfluoroarene materials are approximately 2-D lattices (e.g., $M = 2.2$ for C1) while typical composite materials and polymers containing covalently incorporated chromophores are approximately 3-D lattices (e.g., $M = 2.9$ for the PSLD_33 dendrimer; $\langle P_2 \rangle = 0.019$, $\langle \cos^3\theta \rangle = 0.063$). Note that for PSLD_33 (and for a variety of chromophore-polymer composite materials) $M \sim 3$ was determined with exactly the same measurements and analysis applied to the C1 (and HDFD class materials). Thus, there is strong internal consistency in the defined lattice dimensionalities.

Figure 7. On the left is a cartoon simulation illustrating the relative order for strong interactions and on the right VASE experimental results are shown that support the orthogonal orientation of chromophore and coumarin moieties suggested on the left.



The $|\Delta S^*|$ associated with transitions to phases of reduced dimensionality is approximately 50 kcal for the C1 and arene-perfluoroarene materials. Optimum poling efficiency is observed (by *in situ* monitoring of the introduction of electro-optic activity employing the Teng-Man technique [95,96]) at the temperature corresponding to minimum entropy or maximum order (from IFA data). The cooperativity lengths (ξ), defined by combining IFA and DRS data, are on the order of 100 nm. Combining theoretical calculations with experimental data suggests that the combination of pendant (coumarin or arene-perfluoroarene) and chromophore-chromophore interactions work together to define molecular cooperativity and lattice dimensionality. Theory suggests that other van der Waals interactions make relatively minor contributions. The pendant interactions are approximately twice as important as the chromophore dipole interactions to defining ΔS^* for C1 and HDFD. Atomistic and pseudo-atomistic MD calculations clearly indicate finite autocorrelation functions for coumarin-coumarin, chromophore-chromophore, and coumarin-chromophore interactions consistent with experimental observations. The detailed discussion of MD calculations on C1 and other MAP materials is beyond the scope of this review; however, it can be stated that order and viscoelastic measurements together with MD theoretical calculations provide a very self-consistent picture of the role of nano-engineered pendant interactions in enhancing poling efficiency and EO activity. The pendant interactions both improve acentric order (through reduction of lattice dimensionality) and permit realization of high chromophore number densities. Both of these factors contribute to the observed enhanced electro-optic activity. This research suggests that stronger and better positioned pendant interactions will be required to reduce lattice dimensionality below 2-D and to dramatically enhance (e.g., by a factor of approximately 3–4) acentric order. It is practically impossible to go to significantly higher number densities.

Chromophore guests can be added to the pendant materials discussed above further enhancing electro-optic activity through the additional interactions operative for BCOGs. In some cases, LAP enhancement is possible. The next logical step with respect to chromophore modification is the highly selective introduction of hydrogen bonding and/or ionic interactions.

It is useful to summarize and generalize the observations of this section. In comparing different classes of materials it is useful to discuss poling efficiency, r_{33}/E_{pol} rather than r_{33} , as a figure of merit. The reason for this is that r_{33} will depend on poling configuration (e.g., parallel plate, coplanar electrode, corona poling) and on factors such as the resistivity of poling electrodes (e.g., gold, indium tin oxide, doped silicon, *etc.*). Moreover, the dielectric breakdown of silicon can limit poling voltages to a few tens of volts/micron. The ratio r_{33}/E_{pol} basically indicates how the chromophores of the material respond to a given voltage across the material. Even comparison based on this parameter is not without problems but is probably the most reliable of various alternatives. Values of r_{33}/E_{pol} will depend upon chromophore hyperpolarizability thus we must compare across classes of materials using the same chromophore (molecular first hyperpolarizability). Typically, comparisons (for chromophores with optimized shapes) will be made for the core chromophores of Figure 1. For chromophore-polymer composite materials, such as YLD156 in PMMA poling efficiencies at low chromophore concentrations (in region where r_{33} is linear with N) will typically lie in the range 0.4–0.8 nm²/V² (*i.e.*, for a poling voltage of 100 V/microns, r_{33} values in the range 40–80 pm/V would be expected if such a poling field can be reached). For chromophore-polymer composite materials, the poling efficiency will decrease at higher concentrations because of centrosymmetric ordering of chromophores. For example, for the YLD156 chromophore in PMMA at a concentration of $\sim 4 \times 10^{20}$ molecules/cc (the

concentration of the chromophore in C1), the poling efficiency decreases to $0.15 \text{ nm}^2/\text{V}^2$. For comparison the poling efficiency of the PSLD_33 dendrimer is $1.4 \text{ nm}^2/\text{V}^2$ and covalently incorporated chromophores in site-isolated dendrimers lie in the range $1\text{--}1.5 \text{ nm}^2/\text{V}^2$. For a typical MAP material such as C1, the poling efficiency is $\sim 2 \text{ nm}^2/\text{V}^2$. For this class of materials, values can vary widely depending on the strength of the intermolecular electrostatic interactions among pendant (dendron) moieties. BCOG MAP materials typically exhibit the largest poling efficiencies, e.g., $3\text{--}6 \text{ nm}^2/\text{V}^2$ yielding maximum obtainable electro-optic coefficients in the range $250\text{--}500 \text{ pm/V}$ for simple thin films. The high poling efficiencies of MAP and BCOG MAP materials is a combination of high number density and reduced-dimensionality-enhanced acentric order parameters. LAP can also produce poling efficiencies approaching this range although photo-induced conductivity tends to attenuate efficiency.

It is also useful to attempt to visualize the effect of MAP interactions on lattice dimensionality. Molecular dynamics simulations provide autocorrelation functions for the orientation and interaction of various components of the material including relative to the poling field. Simulations also provide snapshot pictures of the distributions of molecules. However, since the order is relatively low and since order is statistical, it is difficult to envision structures. At any rate, the detailed discussions of the pictures provided by statistical mechanical (MD) simulations for the large number of materials studied is beyond the scope of this review. Theory does permit one to turn up (or down) the strengths of interactions artificially and envision limiting structures. For example, for weak interactions, chromophores and pendants will be nearly randomly oriented. In the accompanying Figure 7, we show the “cartoon” (since it doesn’t correspond to real material intermolecular interaction strengths) limiting form of the structure of C1 for the strong interaction limit.

In the next section, we provide more details regarding processing and characterization techniques.

3. Advances in Materials Processing and Characterization

Individual device applications will define the choice of OEO material used and processing protocols that will be executed in the fabrication of devices. There is a great diversity of applications and device structures developed for those applications and no one material or processing strategy will satisfy all applications. This is a great advantage of OEO materials in that they can be adapted by design to be compatible with a wide range of device structures and are amenable to a wide array of processing protocols.

As already noted, OEO materials can be processed either from solution or the vapor phase although solution processing (spin casting of a thin film followed by electric field poling of the material near its glass transition temperature) has been the far more heavily utilized approach. Materials can also be prepared by sequential synthesis/self-assembly techniques and by crystal growth including from solution, the melt and the vapor phase [97-107]; however, these approaches have not been as widely adapted to the fabrication of prototype devices as have electric field poling methods.

Electric poling has been achieved by parallel plate and coplanar electrode structures and by corona poling. As already noted, electric field poling can be augmented by laser-assisted poling for some materials. A variety of electrode materials have been employed and choice of electrode material and poling configuration can create problems with conductivity. One approach to reducing conductivity

under poling conditions has been to deposit a 25 to 150 nm thin layer of titanium dioxide between the electrode and the OEO material.

For all-organic devices, polymer cladding layers are typically deposited on top of the OEO film to create a triple stack sandwich consisting of cladding layer-active OEO layer-cladding layer [7,108-114]. The OEO material must be sufficiently hard and inert to the solvent used for cladding deposition that pitting of the OEO layer does not occur. Hardness is also crucial for achieving smooth waveguide walls using reactive ion etching.

An attractive feature of OEO/silicon photonic hybrid devices is their simplicity of fabrication. These frequently consist of a simple OEO layer deposited on top of the silicon waveguide structure. When integrating OEO materials with silicon nitride device structures care must be paid to control of material index of refraction but otherwise OEO materials exhibit good compatibility with silicon nitride as well as silicon.

Both electrode (parallel plate or coplanar) and corona poling have been used to induce acentric order although electrode poling has been increasingly utilized. Electrode materials have typically consisted of gold (Au) or indium tin oxide (ITO) although doped silicon (Si) has been employed with silicon photonic device structures. The resistivity of electrode materials is an important factor in defining device bandwidth. Modest conductivity of poorly doped Si can also reduce poling efficiency.

Diels-Alder/Retro-Diels-Alder chemistry can be important in controlling material glass transition temperatures, which is important in processes such as nanoimprint lithography and for optimizing poling efficiency and the thermal stability of poling-induced electro-optic activity. The choice of processing protocols is frequently defined by device structure and intended application. Thus, the reader is referred to other reviews for more detailed discussion of a number of examples [7,108-114].

A few words need to be said regarding advances in materials characterization. Clearly, if theory guiding the nano-engineering of OEO materials is to be tested realistically, improved accuracy and the reliability in the measurement of order parameters needs to be achieved. Most of the characterization improvements of the past several years deal with improved measurement of acentric and centric order parameters. The acentric order parameter cannot be measured directly but can be accessed by measurements of r_{33} or the ratio r_{33}/r_{13} making use of theory to estimate the anisotropy of the first molecular hyperpolarizability tensor. For the most simple systems considered here, the anisotropy of β can be approximately defined by a parameter $b = \{\beta_{zxx} + \beta_{zyy}\}/\beta_{zzz}$. Defining $\Theta = \langle \cos \theta \rangle / \langle \cos^3 \theta \rangle$, where θ is the angle between the poling field and the molecular axis of the dipolar chromophore, the equation for the ratio can be approximately written as:

$$\frac{r_{33}}{r_{13}} = \frac{\chi_{zzz}}{\chi_{xxz}} = \frac{\langle \cos^3 \theta \rangle + b \frac{3}{2} \langle \sin^2 \theta \cos \theta \rangle}{\frac{1}{2} \left\{ \langle \sin^2 \theta \cos \theta \rangle + b \left[\langle \cos \theta \rangle - \frac{3}{2} \langle \sin^2 \theta \cos \theta \rangle \right] \right\}}$$

$$\frac{\langle \sin^2 \theta \cos \theta \rangle}{\langle \cos^3 \theta \rangle} = \frac{\langle \cos \theta \rangle}{\langle \cos^3 \theta \rangle} - 1 = \Theta - 1 \quad (1)$$

$$\frac{r_{33}}{r_{13}} = \frac{2 + 3b\{\Theta - 1\}}{\Theta - 1 + b\{\Theta - \frac{3}{2}(\Theta - 1)\}} = \frac{2 + 3b\{\Theta - 1\}}{\Theta - 1 + \frac{1}{2}b\{3 - \Theta\}}$$

This is an over-simplified result but will be useful for certain materials of interest here. Providing that b can be determined from quantum mechanics and/or estimated by applied electric field HRS and EFISH measurements, Θ can be obtained from r_{33}/r_{13} measurements. The greatest uncertainty in extracting the acentric order parameter from electro-optic measurements relates to the uncertainty in b . It is also important to cross compare various techniques for measurement of the elements of the electro-optic tensor. For a given measurement technique, errors can arise from failing to employ an analysis that takes into account all of the features of a particular measurement. The analysis of the Teng-Man by Hermann and coworkers [96] is an example of this problem. Our approach has been to employ a variety of measurement techniques mentioned in the last section and to develop a more sophisticated analysis of the ATR experiment.

In like manner, characterization of the centric order parameter, $\langle P_2 \rangle$, requires some improvement in measurement techniques. We have improved on the VAPAS technique of Graf and coworkers [115] by measuring the dependence of the ratio of “p” and “s” absorption on angular variation. We refer to this modification as VAPRAS [92]. As discussed in detail elsewhere [92], utilizing the ratio of p and s absorption takes out many of the experimental artifacts associated with a measurement using p-polarized light alone. Because our samples are strongly absorbing we employ full Jones matrix analysis of data [116].

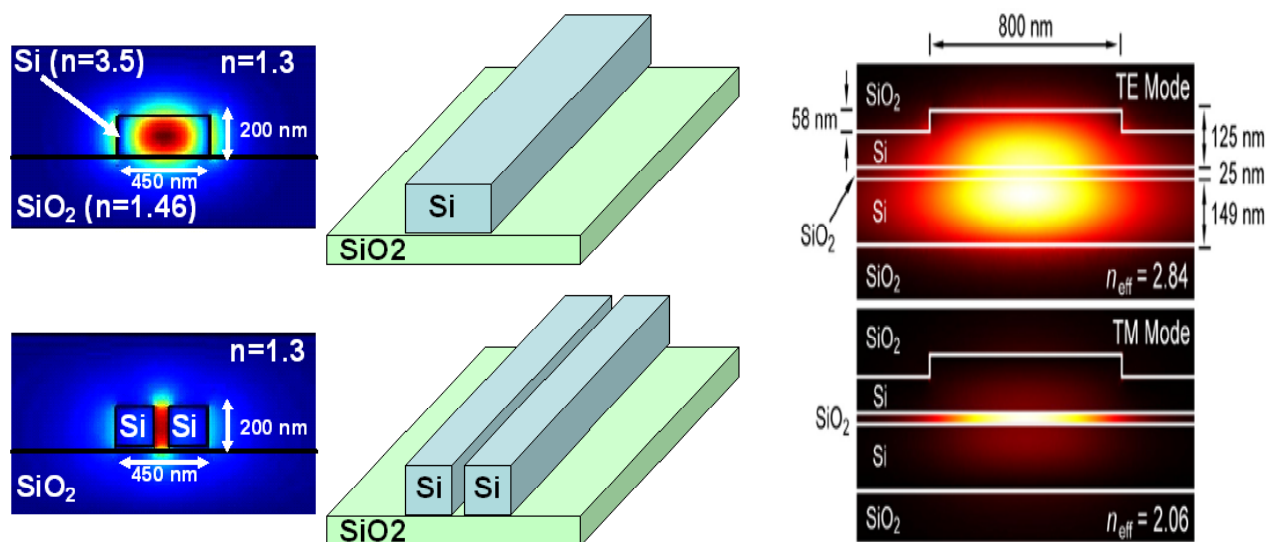
4. Devices

As with the diversity of materials processing and characterization options, a diverse array of devices and device architectures have been explored. As all-organic devices have been reviewed recently [117], we limit this discussion to two relatively new areas of focus on devices; namely, (1) slotted silicon photonic devices and (2) plasmonic/photonic crystal/metamaterial devices.

Basically, four classes of hybrid OEO/silicon photonic stripline and ring microresonator devices have been explored. The first simply involves over coating a silicon waveguide with OEO material. Modulation of light propagating in the silicon waveguide is effected by modulation of the evanescent field. Lipson [33] motivated interest in slotted structures by showing that light could be concentrated in low index of refraction slots cut into silicon waveguides (see accompanying Figure 8). This permitted a dramatic enhancement of optical fields and because of the potential of reduced electrode dimensions there was also the potential for significant enhancement of low frequency fields including the poling field. Both vertical and horizontal slot structures (see Figure 8) have been demonstrated with the vertical slot structures much easier to fabricate. The main advantage of the horizontal slot structure is the convenient deposition surface that exists for this structure.

Most recently, nanowire or rib structures have been fabricated. This device structure also exploits modulation of the evanescent field in the OEO material that is spun on top of a silicon rib structure. Sub-1 volt modulation has been realized for slotted structures and these likely define the state-of-the-art for second order optical nonlinearity-defined device performance (electro-optic modulation and switching, optical rectification, and difference frequency generation).

Figure 8. Nanoscopic silicon photonic waveguides including vertical and horizontal slot waveguides, together with computed mode profiles, are shown.

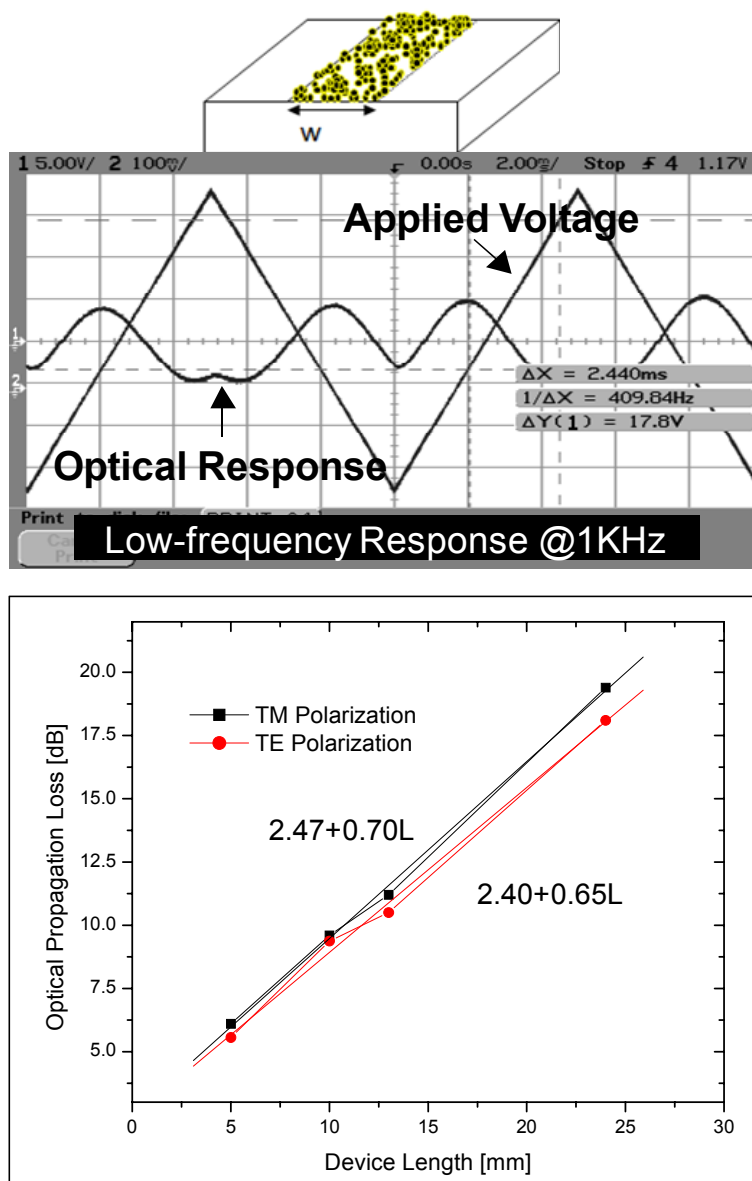


The major problems with devices involving incorporation of OEO materials into plasmonic, photonic crystal (slow light), and metamaterial device architectures involve optical loss and bandwidth limitation. As already noted in this review, some intriguing prototype devices have been demonstrated.

For hybrid OEO/plasmonic devices, it has been possible to reduce optical loss by employing nanostructured gold and silver metal films rather than utilizing solid films. Utilization of nanostructured metal films permits the systematic variation of contributions made by long range surface modes (LRSM) and long range surface plasmonic polaritons (LRSP). Consideration of both solid and nanostructured metal films has been pursued for a variety of simple device structure (e.g., Mach Zehnder modulators and phased modulators employing insulator-metal-insulator (IMI) and metal-insulator-metal (MIM) architectures) and more sophisticated structures (optical signal processors, optical SSB modulators, 4 channel RF phase shifters, linearized double channel MZ modulators) [48,49,118]. The dependence of performance on film thickness (*i.e.*, the relative contributions made by LRSMs and LRSP) has been investigated. The major advantage of nanostructured metal films is the ability to control optical loss and to achieve short (e.g., ~ 1 cm or less) device lengths. We have explored OEO hybrid plasmonic devices for both simple composite (e.g., YLD146 in APC) and binary chromophore organic glasses. Some representative results are shown in Figure 9 for simple Mach Zehnder amplitude and single channel phase modulators. For a 1.5 cm. Mach Zehnder IMI modulator based on nanostructured gold films of 1 nm thickness, a driving voltage (at 1,550 nm optical wavelength) of 4 volts was observed for single arm driving (2 volts for push-pull driving).

For a 0.8 cm. interaction length phase modulator employing nanostructured gold films of 2 nm thickness, a driving voltage of 5.4 volts was observed operating at an optical wavelength of 1,550 nm. Sub- λ concentration of light has also been demonstrated for EO-active plasmonic waveguide structures.

Figure 9. The electro-optic modulation and optical loss characteristics are shown for a nanostructured gold thin (1 nm) film IMI structure. The optical propagation loss was observed to be 0.65–0.70 dB/mm at 1,550 nm. The measured insertion loss was 14 dB.



4. Conclusions

Nano-engineering of chromophore structures has been shown to permit control of intermolecular electrostatic interactions that influence electric field poling efficiency. Electro-optic activity greater than that expected for chromophores behaving independently (chromophores experiencing no intermolecular electrostatic interactions), has been demonstrated. Incorporated-by-design interactions (coumarin-coumarin and arene-perfluoroarene) can influence lattice dimensionality and nanoviscoelastic properties. Lattice dimensionality can be defined by investigation of acentric and centric order parameters and their ratio. Record electro-optic activity is observed for binary chromophore organic glasses utilizing nano-engineered chromophore-containing host materials.

Correlated quantum and statistical mechanics methods afford quantitative investigation of the effects of a wide range of intermolecular interactions and permit understanding of the factors that define electro-optic activity in all classes of materials studied to the present.

The compatibility of OEO materials with a diverse range of materials and their ease of integration into a diverse range of device structures has motivated incorporation of these materials into a wide variety of device structures including slotted and nanowire silicon photonic, plasmonic, and metamaterial devices. Prototype device performance results are very promising, particularly for hybrid OEO/silicon (and silicon nitride) devices.

Because of the enormous number of publications dealing with OEO materials over the past two-plus decades a comprehensive review of the literature is not possible here. The reader is referred to the cited reviews for more comprehensive coverage.

Acknowledgements

The authors gratefully acknowledge financial support from the National Science Foundation (DMR00905686) and the Air Force Office of Scientific Research (FA9550-09-1-0589). The authors also wish to thank members of Robinson, Overney, Jen, Reid, and Dalton research groups at the University of Washington for many helpful discussions and with assistance with calculations and measurements.

References and Notes

1. Hochberg, M.; Baehr-Jones, T.; Wang, G.; Shearn, M.; Harvard, K.; Liu, J.; Chen, B.; Shi, Z.; Lawson, R.; Sullivan, P.A.; *et al.* All optical modulator in silicon with terahertz bandwidth. *Nat. Mater.* **2006**, *5*, 703-709.
2. Baehr-Jones, T.; Hochberg, M.; Wang, G.; Lawson, R.; Liao, Y.; Sullivan, P.A.; Dalton, L.R.; Jen, A.K.-Y.; Scherer, A. Optical modulation and detection in slotted silicon waveguides. *Opt. Express* **2005**, *13*, 5216-5226.
3. McLaughlin, C.V.; Hayden, L.M.; Polishak, B.; Huang, S.; Luo, J.; Kim, T.D.; Jen, A.K.-Y. Wideband 15-THz response using organic electrooptic emitter-sensor pairs at telecommunication wavelengths. *Appl. Phys. Lett.* **2008**, *92*, 151107-1-3.
4. Drener, K.A.; Larsen, R.J.; Strohkendl, F.P.; Dalton, L.R. Femtosecond, frequency-agile, phase-sensitive-detected multi-wave-mixing nonlinear optical spectroscopy applied to p-electron photonic materials. *J. Phys. Chem.* **1999**, *103*, 2290-2301.
5. Lee, M.; Katz, H.E.; Erben, C.; Gill, D.M.; Gopalan, P.; Heber, J.D.; McGee, D.J. Broadband modulation of light using an electro-optic polymer. *Science* **2002**, *298*, 1401-1403.
6. Chen, D.; Fetterman, H.R.; Chen, A.; Steier, W.H.; Dalton, L.R.; Wang, W.; Shi, Y. Demonstration of 110 GHz electro-optic polymer modulators. *Appl. Phys. Lett.* **1997**, *70*, 3335-3337.
7. Dalton, L.R.; Harper, A.W.; Ren, A.S.; Wang, F.; Todorova, G.; Chen, J.; Zhang, C.; Lee, M. From chromophore design to integration with semiconductor VLSI electronics and silica fiber optics. *Ind. Eng. Chem. Res.* **1999**, *38*, 8-33.

8. Kim, T.-D.; Luo, J.; Cheng, Y.-J.; Shi, Z.; Hau, S.; Jang, S.-H.; Zhou, X.-H.; Tian, Y.; Polishak, B.; Hunag, S.; *et al.* Binary chromophore systems in nonlinear optical dendrimers and polymers for large electrooptic activities. *J. Phys. Chem. C* **2008**, *112*, 8091-8098.
9. Dalton, L.R.; Harper, A.W.; Robinson, B.H. The role of London forces in defining noncentrosymmetric order of high dipole moment-high hyperpolarizability chromophores in electrically poled polymeric thin films. *Proc. Natl. Acad. Sci. USA* **1997**, *94*, 4842-4847.
10. Dalton, L.R.; Robinson, B.H.; Jen, A.K.-Y.; Steier, W.H.; Neilsen, R. Systematic development of high bandwidth, low drive voltage organic electro-optic devices and their applications. *Opt. Mater.* **2003**, *21*, 19-28.
11. Robinson, B.H.; Dalton, L.R. Monte Carlo statistical mechanical simulations of the competition of intermolecular electrostatic and poling field interactions in defining macroscopic electro-optic activity for organic chromophore/polymer materials. *J. Phys. Chem. A* **2000**, *104*, 4785-4795.
12. Shi, Y.; Zhang, C.; Zhang, H.; Bechtel, J.H.; Dalton, L.R.; Robinson, B.H.; Steier, W.H. Low (sub-1 volt) halfwave voltage polymeric electrooptic modulators achieved by control of chromophore shape. *Science* **2000**, *288*, 119-122.
13. Benight, S.J.; Johnson, L.E.; Barnes, R.; Olbricht, B.C.; Bale, D.H.; Eichinger, B.E.; Dalton, L.R.; Sullivan, P.A.; Robinson, B.H. Reduced dimensionality in organic electro-optic materials. *J. Phys. Chem. B* **2010**, *114*, 11949-11956.
14. Dalton, L.R.; Benight, S.J.; Johnson, L.E.; Knorr, D.B., Jr.; Kosilkin, I.; Eichinger, B.E.; Robinson, B.H.; Jen, A.; Overney, R. Systematic nano-engineering of soft matter organic electro-optic materials. *Chem. Mater.* **2011**, *23*, 430-445.
15. Cho, M.J.; Choi, D.H.; Sullivan, P.A.; Akelaitis, A.J.P.; Dalton, L.R. Recent progress in second-order nonlinear optical polymers and dendrimers. *Prog. Polym. Sci.* **2008**, *33*, 1013-1058.
16. Dalton, L.R.; Sullivan, P.A.; Bale, D.H. Electric field poled organic electro-optic materials: State of the art and future prospects. *Chem. Rev.* **2010**, *110*, 25-55.
17. Budy, S.M.; Suresh, S.; Spraul, B.K.; Smith, D.W. High-temperature chromophores and perfluorocyclobutyl copolymers for electro-optic applications. *J. Phys. Chem. C* **2008**, *112*, 8089-8104.
18. Luo, J.; Haller, M.; Li, H.; Kim, T.-D.; Jen, A.K.-Y. Highly efficient and thermally stable electro-optic polymer from a smartly controlled crosslinking process. *Adv. Mater.* **2003**, *15*, 1635-1638.
19. Luo, J.; Huang, S.; Shi, Z.; Polishak, B.M.; Zhou, X.-H.; Jen, A.K.-Y. Tailored organic electro-optic materials and their hybrid systems for device applications. *Chem. Mater.* **2011**, *23*, 544-553.
20. Luo, J.D.; Kim, T.D.; Jen, A.K.-Y. Unprecedented Electro-Optic Properties in Polymers and Dendrimers Enabled by "Click Chemistry" Based on the Diels-Alder Reactions. In *Click Chemistry for Biotechnology and Materials Science*; Lahann, J., Ed.; John Wiley & Sons: New York, NY, USA, 2009; pp. 379-397.
21. Shi, Z.; Liang, W.; Luo, J.D.; Huang, S.; Polishak, B.M.; Li, X.; Younkin, T.R.; Block, B.A.; Jen, A.K.-Y. Tuning the kinetics and energetic of Diels-Alder cycloaddition reactions to improve poling efficiency and thermal stability of high temperature crosslinked electro-optic polymers. *Chem. Mater.* **2010**, *22*, 5601-5608.

22. Mao, S.S.H.; Ra, Y.; Guo, L.; Zhang, C.; Dalton, L.R.; Chen, A.; Garner, S.M.; Steier, W.H. Progress towards device-quality second-order nonlinear optical materials: 1. Influence of composition and processing conditions on nonlinearity, temporal stability, and optical loss. *Chem. Mater.* **1998**, *10*, 146-155.
23. Chen, A.; Chuyanov, V.; Marti-Carrera, F.I.; Garner, S.M.; Steier, W.H.; Chen, J.; Sun S.S.; Dalton, L.R. Vertically tapered polymer waveguide mode size transformer for improved fiber coupling. *Opt. Eng.* **2000**, *39*, 1507-1516.
24. Oh, M.S.; Zhang, C.; Lee, H.J.; Steier, W.H.; Fetterman, H.R. Low-loss interconnection between electrooptic and passive polymer waveguides with a vertical taper. *IEEE Photon. Technol. Lett.* **2002**, *14*, 1121-1123.
25. Zang, D.Y.; Shu, G.; Downing, T.; Lin, W.; Oh, C.; Bechtel, J. Insertion loss reduction in high speed polymer electrooptic modulators using tapered waveguide, fiber tip lenses and modification of waveguide structures. *Proc. SPIE* **2003**, *4991*, 601-609.
26. Chang, D.H.; Azfar, T.; Kim, S.K.; Fetterman, H.R.; Zhang, C.; Steier, W.H. Vertical adiabatic transition between silica planar waveguide and electro-optic polymer fabricated using grayscale lithography. *Opt. Lett.* **2003**, *28*, 860-871.
27. Enami, Y.; Meredith, G.; Peyghambarian, N.; Kawazu, M.; Jen, A.K.-Y. Hybrid electro-optic polymer and selectively buried sol-gel waveguides. *Appl. Phys. Lett.* **2003**, *82*, 490-492.
28. DeRose, C.T.; Himmelhuber, R.; Mathine, D.; Norwood, R.A.; Jen, A.K.-Y.; Peyghambarian, N. High Δn strip-loaded electro-optic polymer waveguide modulators with low optical insertion loss. *Opt. Express* **2009**, *17*, 3316-3321.
29. Araci, I.E.; Himmelhuber, R.; DeRose, C.T.; Luo, J.D.; Jen, A.K.-Y.; Norwood, R.A.; Peyghambarian, N. Alignment-free fabrication of a hybrid electro-optic polymer/ion-exchange glass coplanar modulator. *Opt. Express* **2010**, *18*, 21038-21046.
30. Huang, Y.; Paloczi, G.T.; Yariv, A.; Zhang, C.; Dalton, L.R. Fabrication and replication of polymer integrated optical devices using electron-beam lithography and soft lithography. *J. Phys. Chem. B* **2004**, *108*, 8606-8613.
31. Song, H.-C.; Oh, M.-C.; Ahn, S.-W.; Steier, W.H. Flexible low-voltage electro-optic polymer modulators. *Appl. Phys. Lett.* **2003**, *82*, 4431-4434.
32. Garner, S.M.; Lee, S.-S.; Chuyanov, V.; Chen, A.; Yacoubian, A.; Steier, W.H.; Dalton, L.R. Three dimensional integrated optics using polymers. *IEEE J. Quantum Electron.* **1999**, *35*, 1146-1155.
33. Xu, Q.; Almeida, V.R.; Panepucci, R.R.; Lipson, M. Experimental demonstration of guiding and confining light in nanometer-size low-refractive-index material. *Opt. Lett.* **2004**, *20*, 1626-1628.
34. Takayesu, J.; Hochberg, M.; Baehr-Jones, T.; Chan, E.; Wang, G.; Sullivan, P.A.; Liao, Y.; Davies, J.; Dalton, L.R.; Scherer, A.; Krug, W. A hybrid electro-optic microring resonator-based $1 \times 4 \times 1$ ROADM for wafer scale optical interconnects. *IEEE J. Lightwave Technol.* **2008**, *27*, 440-448.
35. Baehr-Jones, T.; Penkov, B.; Huang, J.; Sullivan, P.A.; Davies, J.; Takayesu, J.; Luo, J.; Kim, T.-D.; Dalton, L.R.; Jen, A.K.-Y.; *et al.* Nonlinear polymer-clad silicon slot waveguide modulator with a half wave voltage of 0.25 V. *Appl. Phys. Lett.* **2008**, *92*, 163303-1-3.
36. Block, B.A.; Younkin, T.R.; Reshotko, R.; Chang, P.; Luo, L.D.; Jen, A.K.-Y. Electro-optic polymer cladding ring resonator modulators. *Opt. Express* **2008**, *16*, 18326-18333.

37. Ding, R.; Baehr-Jones, T.; Liu, Y.; Bojko, R.; Witzens, J.; Huang, S.; Luo, J.; Benight, S.; Sullivan, P.; Fedeli, J.-M.; *et al.* Demonstration of a low $V_{\pi}L$ modulator with GHz bandwidth based on an electro-optic polymer-clad silicon slot waveguide. *Opt. Express* **2010**, *18*, 15618-15623.
38. Ding, R.; Baehr-Jones, T.; Kim, W.-J.; Spott, A.; Fournier, M.; Fedeli, J.-M.; Huang, S.; Luo, J.; Jen, A.K.-Y.; Dalton, L.R.; *et al.* Sub-volt silicon-organic electrooptic modulator with 500 MHz bandwidth. *IEEE/OSA J. Lightwave Technol.* **2011**, *29*, 1112-1117.
39. Gould, M.; Baehr-Jones, T.; Ding, R.; Huang, S.; Luo, J.; Jen, A.K.-Y.; Fedeli, J.-M.; Fournier, M.; Hochberg, M. Silicon-polymer hybrid slot waveguide ring-resonator modulator. *Opt. Express* **2011**, *19*, 3952-3961.
40. Lin, C.-Y.; Wang, X.; Chakravarty, S.; Lee, B.S.; Lai, W.; Luo, J.; Jen, A.K.-Y.; Chen, R.T. Electro-optic polymer infiltrated silicon photonic crystal slot waveguide modulator with 23 dB slow light enhancement. *Appl. Phys. Lett.* **2010**, *97*, 093304-1-3.
41. Wang, X.; Lin, C.-Y.; Chakravarty, S.; Luo, J.; Jen, A.K.-Y.; Chen, R.T. Effective in-device r_{33} of 735 pm/V on electro-optic polymer infiltrated silicon photonic crystal slot waveguides. *Opt. Lett.* **2011**, *36*, 882-884.
42. Wulbern, J.H.; Hampe, J.; Petrov, A.; Eich, M.; Luo, J.D.; Jen, A.K.-Y.; Falco, A.D.; Krauss, T.F.; Bruns, J.; Ptermann, K. Electro-optic modulation in slotted resonant photonic crystal heterostructures. *Appl. Phys. Lett.* **2009**, *94*, 241107-1-3.
43. Wulbern, J.H.; Prorok, S.; Hampe, J.; Petrov, A.; Eich, M.; Luo, J.; Jen, A.K.-Y.; Jenett, M.; Jacob, A. 40 GHz electro-optic modulation in hybrid silicon-organic slotted photonic crystal waveguides. *Opt. Lett.* **2010**, *35*, 2753-2755.
44. Wulbern, J.H.; Petrov, A.; Eich, M. Electro-optic modulator in a polymer infiltrated silicon slotted photonic crystal waveguide heterostructure resonator. *Opt. Express* **2009**, *17*, 304-313.
45. Koos, C.; Vorreau, P.; Vallaitis, T.; Dumon, P.; Bogaerts, W.; Baets, R.; Esembeson, B.; Biaggio, I.; Michinobu, T.; Diederich, F.; *et al.* All-optical high-speed signal processing with silicon-organic hybrid slot waveguides. *Nat. Photonics* **2009**, *3*, 216-219.
46. Leuthod, J.; Freude, W.; Brosi, J.-M.; Baets, R.; Dumon, P.; Biaggio, I.; Scimeca, M.L.; Diederich, F.; Frank, B.; Koos, C. Silicon organic hybrid technology—A platform for practical nonlinear optics. *Proc. IEEE* **2009**, *97*, 1304-1316.
47. Figi, H.; Bale, D.H.; Szep, A.; Dalton, L.R.; Chen, A. Electro-optic modulation in horizontally slotted silicon/organic crystal hybrid devices. *J. Opt. Soc. Am. B* **2011**, in press.
48. Kim, S.-K.; Sylvain, N.; Benight, S.J.; Kosilkin, I.; Bale, D.H.; Robinson, B.H.; Geary, K.; Jen, A.K.-Y.; Steier, W.H.; Fetterman, H.R.; *et al.* Active plasmonic and metamaterial devices. *Proc. SPIE* **2010**, *7754*, 775403.
49. Dalton, L.R.; Jen, A.K.-Y.; Robinson, B.H.; Overney, R.; Benight, S.J.; Knorr, D.B., Jr.; Kim, S.-K.; Fetterman, H.R.; Zhang, C. Optimization of organic NLO materials for integration with silicon photonic, plasmonic (metal optics), and metamaterial devices. *Proc. SPIE* **2011**, *7935*, 793502.
50. Shi, S.; Prather, D.W. Ultrabroadband electro-optic modulator based on hybrid silicon-polymer dual vertical slot waveguide. *Adv. Optoelectron.* **2011**, *2011*, 714895.
51. Shi, S.; Prather, D.W. Dual rf-optical slot waveguide for ultrabroadband modulation with a subvolt V_{π} . *Appl. Phys. Lett.* **2010**, *96*, 201107-1-3.

52. Huang, S.; Kim, T.-D.; Luo, J.D.; Hau, S.; Cheng, Y.-J.; Zou, J.; Shi, Z.; Zhou, X.-H.; Jen, A.K.-Y. Large electro-optic coefficients form enhanced poling of nonlinear optical polymers using a thin TiO₂-modified transparent electrode. *Appl. Phys. Lett.* **2010**, *96*, 243311-1-3.
53. Bale, D.; Liang, W.; Dalton, L.R.; Reid, P.; Robinson, B.; Eichinger, B.; Li, X. Dielectric dependence of the first molecular hyperpolarizability for electro-optic chromophores. *J. Phys. Chem. B* **2011**, *115*, 3505-3513.
54. Johnson, L.E.; Barnes, R.; Draxler, T.W.; Eichinger, B.E.; Robinson, B.H. Dielectric constants of simple liquids: Stockmayer and ellipsoidal fluids. *J. Phys. Chem. B* **2010**, *114*, 8431-8440.
55. Takimoto, Y.; Isborn, C.M.; Eichinger, B.E.; Rehr, J.J.; Robinson, B.H. Frequency and solvent dependence of nonlinear optical properties. *J. Phys. Chem. C* **2008**, *112*, 8016-8221.
56. Takimoto, Y.; Vila, F.D.; Rehr, J.J. Real-time, time-dependent density functional theory approach for frequency-dependent nonlinear optical response in photonic molecules. *J. Chem. Phys.* **2007**, *127*, 154114-10.
57. Takimoto, Y. A Real-Time Time-Dependent Density Functional Theory Method for Calculating Linear and Nonlinear Dynamic Optical Response. Ph.D. Dissertation, University of Washington, Seattle, WA, USA, 2008.
58. Kim, W.-K.; Hayden, L.M. Fully atomistic modeling of an electric field poled guest-host nonlinear optical polymer. *J. Chem. Phys.* **1999**, *111*, 5212-5222.
59. Leahy-Hoppa, M.R.; French, J.; Cunningham, P.D.; Hayden, L.M. Atomistic Molecular Modeling of Electric Field Poling of Nonlinear Optical Polymers. In *Nonlinear Optical Properties of Matter: From Molecules to Condensed Phases*; Papadopoulos, M.G., Leszczynski, J., Sadlej, A.J., Eds.; Kluwer Press: New York, NY, USA, 2006; pp. 337-357.
60. Leahy-Hoppa, M.R.; Cunningham, P.D.; French, J.A.; Hayden, L.M. Atomistic molecular modeling of the effect of chromophore concentration on the electro-optic coefficient in nonlinear optical polymers. *J. Phys. Chem. A* **2006**, *110*, 5792-5797.
61. Makowska-Janusik, M.; Reis, H.; Papadopoulos, M.G. Molecular dynamics simulation of electric field poled nonlinear optical chromophores incorporated in a polymer matrix. *J. Phys. Chem. B* **2004**, *108*, 588-596.
62. Neilsen, R.; Rommel, H.; Robinson, B. Simulation of the loading parameter in organic nonlinear optical materials. *J. Phys. Chem.* **2004**, *108*, 8659-8667.
63. Rommel, H.L.; Robinson, B.H. Orientation of electro-optic chromophores under poling conditions: A spheroidal model. *J. Phys. Chem. C* **2007**, *111*, 18765-18777.
64. Pereverzev, Y.V.; Gunnerson, K.N.; Prezhdo, O.V.; Sullivan, P.A.; Liao, Y.; Olbricht, B.C.; Akelaitis, A.J.P.; Jen, A.K.-Y.; Dalton, L.R. Guest-host cooperativity in organic materials greatly enhances the nonlinear optical response. *J. Phys. Chem. C* **2008**, *112*, 4355-4363.
65. Sullivan, P.A.; Rommel, H.L.; Takimoto, Y.; Hammond, S.R.; Bale, D.H.; Olbricht, B.C.; Liao, Y.; Rehr, J.J.; Eichinger, B.E.; Jen, A.K.-Y.; *et al.* Modeling the optical behavior of complex organic media: From molecules to materials. *J. Phys. Chem. B* **2009**, *113*, 15581-15588.
66. Johnson, L.E.; Benight, S.J. Monte Carlo and molecular dynamics simulations of coumarin-containing electro-optic dendrimers. to be submitted for publication; see also: Benight, S.J. Nanoengineering of Soft Matter Interactions in Organic Electro-Optic Materials. Ph.D. Thesis, University of Washington, Seattle, WA, USA, 2011.

67. Hammond, S.R.; Clot, O.; Firestone, K.A.; Bale, D.H.; Haller, M.M.; Phelan, G.D.; Carlson, B.; Jen, A.K.-Y.; Reid, P.J.; Dalton, L.R. Site-isolated electro-optic chromophores based on substituted 2,2'-Bis(3,4-propylenedioxythiophene) π -conjugated bridges. *Chem. Mater.* **2008**, *20*, 3425-3434.
68. Cheng, Y.-J.; Luo, J.; Hunag, S.; Zhou, X.-H.; Shi, Z.; Kim, T.-D.; Bale, D.H.; Takahasi, S.; Yick, A.; Polishak, B.M.; *et al.* Donor-acceptor thiolated polyenic chromophores exhibiting large optical nonlinearity and excellent photostability. *Chem. Mater.* **2008**, *20*, 5047-5054.
69. Hammond, S.R.; Siness, J.; Dubbury, S.; Firestone, K.A.; Wawrzak, Z.; Benedict, J.; Clot, O.; Reid, P.; Dalton, L.R. Molecular engineering of nanoscale order in dipolar organic glasses. *J. Mater. Chem.* **2011**, submitted.
70. Shi, Z.; Luo, J.; Huang, S.; Zhou, X.-H.; Kim, T.-D.; Cheng, Y.-J.; Polishak, B.M.; Younkin, T.R.; Jen, A.K.-Y. Reinforced site isolation leading to remarkable thermal stability and high electro-optic activities in crosslinked nonlinear optical dendrimers. *Chem. Mater.* **2008**, *20*, 6372-6377.
71. Zhang, C.; Benight, S.J. Department of Chemistry, University of Washington. Private Communication. 2011.
72. Sullivan, P.A.; Rommel, H.; Liao, Y.; Olbricht, B.C.; Akelaitis, A.J.P.; Firestone, K.A.; Kang, J.-W.; Luo, J.; Choi, D.H.; Eichinger, B.E.; *et al.* Theory-guided design and synthesis of multi-chromophore dendrimers: An analysis of the electro-optic effect. *J. Am. Chem. Soc.* **2007**, *129*, 7523-7530.
73. Olbricht, B.C.; Sullivan, P.A.; Wen, G.-A.; Mistry, A.; Davies, J.A.; Ewy, T.R.; Eichinger, B.E.; Robinson, B.H.; Reid, P.J.; Dalton, L.R. Laser-assisted poling of binary chromophore materials. *J. Phys. Chem. C* **2008**, *112*, 7983-7988.
74. Kim, S.; Pei, Q.; Fetterman, H.R.; Olbricht, B.C.; Dalton, L.R. Photo-assisted corona poled YLD-124/DR1-co-PMMA electro-optic device using photisomerization. *IEEE Photonics Technol. Lett.* **2011**, *23*, 845-847.
75. Wang, Z.; Sun, W.; Chen, A.; Kosilkin, I.; Bale, D.; Dalton, L.R. Direct-laser assisted poling of vacuum deposited organic electro-optic thin films. *Opt. Lett.* **2011**, *36*, 2853-2855.
76. Gray, T.; Kilgore, J.P.; Luo, J.; Jen, A.K.-Y.; Overney, R.M. Molecular mobility and transitions in complex organic systems studied by shear force microscopy. *Nanotechnology* **2007**, *18*, 044009-1-9.
77. Gray, T.; Kim, T.D.; Knorr, D.B., Jr.; Luo, J.; Jen, A.K.-Y.; Overney, R.M. Mesoscale dynamics and cooperativity of networking dendronized nonlinear optical molecular glasses. *Nano Lett.* **2008**, *8*, 754-739.
78. Knorr, D.B., Jr.; Zhou, X.-H.; Shi, Z.; Luo, J.; Jang, S.-H.; Jen, A.K.-Y.; Overney, R.M. Molecular mobility in self-assembled dendritic chromophore glasses. *J. Phys. Chem. B* **2009**, *112*, 14180-14188.
79. Zhou, X.-H.; Luo, J.; Huang, S.; Kim, T.-D.; Shi, Z.; Cheng, Y.-J.; Jang, S.-H.; Knorr, D.B., Jr.; Overney, R.M.; Jen, A.K.-Y. Supramolecular self-assembled dendritic nonlinear optical chromophores: Fine-tuning of arene-perfluoroarene interactions for ultralarge electro-optic activity and enhanced thermal stability. *Adv. Mater.* **2009**, *21*, 1976-1981.
80. Knorr, D.B., Jr.; Gray, T.O.; Overney, R.M. Intrinsic friction analysis—Novel nanoscopic access to molecular mobility in constrained organic systems. *Ultramicroscopy* **2009**, *109*, 981-1000.

81. Kim, W.H.; Bihari, B.; Moody, R.; Kodali, N.B.; Kumar, J.; Tripathy, S.K. Self-assembled spin-coated bulk films of a novel. *Macromolecules* **1995**, *28*, 642-647.
82. Ribierre, J.C.; Mager, L.; Fort, A.; Mery, S. Effects of viscoelastic properties on the dielectric and electrooptic responses of low-T-g guest-host polymers. *Macromolecules* **2003**, *36*, 2516-2525.
83. Chen, A.; Chuyanov, V.; Garner, S.M.; Steier, W.H.; Dalton, L.R. Modified attenuated total reflection for the fast and routine electrooptic measurements of nonlinear optic polymer thin films. *OSA Tech. Dig. Series Org. Thin Films Photonic Appl.* **1997**, *14*, 158-159.
84. Davies, J.A.; Elangovan, A.; Sullivan, P.A.; Olbricht, B.C.; Bale, D.H.; Ewy, T.R.; Isborn, C.M.; Eichinger, B.E.; Robinson, B.H.; Reid, P.J.; *et al.* Rational enhancement of second-order nonlinearity: Bis-(4-methoxyphenyl)-heteroaryl-amino donor-based chromophores—Design, synthesis, and electro-optic activity. *J. Am. Chem. Soc.* **2008**, *130*, 10565-10575.
85. Jiang, Y.; Cao, Z.; Shen, Q.; Dou, X.; Chen, Y.; Ozaki, Y. Improved attenuated-total-reflection technique for measuring the electro-optic coefficients of nonlinear optical polymers. *J. Opt. Soc. Am. B* **2000**, *17*, 805-808.
86. Kalluri, S.; Garner, S.M.; Ziari, M.; Steier, W.H.; Shi, Y.; Dalton, L.R. Simple two-slit interference electro-optic coefficients measurement technique and efficient coplanar electrode poling of polymer thin films. *Appl. Phys. Lett.* **1996**, *69*, 275-277.
87. Sun, W.W.; Wang, Z.; Chen, A.; Kosilkin, I.; Bale, D.; Lin, L.; Dalton, L.R. Electro-optic thin films of aligned organic nonlinear optic molecules through vacuum deposition. *Opt. Express* **2011**, *19*, 11189-11195.
88. Nagtegaele, P.; Brasselet, E.; Zyss, J. Anisotropy and dispersion of a Pockels tensor: A benchmark for electro-optic organic thin-film assessment. *J. Opt. Soc. Am. B* **2003**, *20*, 1932-1936.
89. Greenlee, C.; Guilmo, A.; Opadeyi, A.; Himmelhuber, R.; Norwood, R.A.; Falahi, M.; Luo, J.D.; Huang, S.; Zhou, X.-H.; Jen, A.K.-Y. Mach-Zehnder interferometry method for decoupling electro-optic and piezoelectric effects in poled polymer films. *Appl. Phys. Lett.* **2010**, *97*, 041109-1-4.
90. Firestone, K.A.; Lao, D.B.; Casmier, D.M.; Clot, O.; Dalton, L.R.; Reid, P.J. Frequency-agile hyper-Rayleigh scattering studies of electro-optic chromophores. *Proc. SPIE* **2005**, *5935*, 59350P1-9.
91. Campo, J.; Desmet, F.; Wenseleers, W.; Goovaerts, E. Highly sensitive setup for tunable wavelength hyper-Rayleigh scattering with parallel detection and calibration data for various solvents. *Opt. Express* **2009**, *17*, 4587-4604.
92. Olbricht, B.C.; Sullivan, P.A.; Davies, J.A.; Dennis, P.C.; Hurst, J.T.; Johnson, L.E.; Bale, D.H.; Benight, S.J.; Hilfiker, J.N.; Chen, A.; *et al.* Measuring order in contact-poled organic electro-optic materials with variable angle polarization-referenced absorption spectroscopy (VAPRAS). *J. Phys. Chem. B* **2011**, *115*, 231-241.
93. Woollam, J.A. Overview of Variable Angle Spectroscopic Ellipsometry (VASE), Part I: Basic Theory and Typical Applications. In *Optical Metrology*; SPIE: Bellingham, WA, USA, 1999; Volume CR72, pp. 3-28.
94. Johs, B. Overview of Variable Angle Spectroscopic Ellipsometry (VASE), Part II: Advanced Applications. In *Optical Metrology*; SPIE: Bellingham, WA, USA, 1999; Volume CR72, pp. 29-58.

95. Teng, C.; Man, H. Simple reflection technique for measuring the electro-optic coefficient of poled polymers. *Appl. Phys. Lett.* **1990**, *56*, 1734-1736.
96. Park, D.H.; Lee, C.H.; Herman, W.N. Analysis of multiple reflection effects in reflective measurements of electro-optic coefficients of poled polymers in multilayer structures. *Opt. Express* **2006**, *14*, 8866-8884.
97. Facchetti, A.; Abboto, A.; Beverina, L.; van der Boom, M.E.; Dutta, P.; Evmenenko, G.; Pagani, G.A.; Marks, T.J. Layer-by-layer self-assembled pyrrole-based donor-acceptor chromophores as electro-optic materials. *Chem. Mater.* **2003**, *15*, 33-38.
98. Facchetti, A.; Annoni, E.; Beverina, L.; Morone, M.; Zhu, P.; Marks, T.J.; Pagani, G.A. Very large electro-optic responses in H-bonded heteroaromatic films grown by physical vapour deposition. *Nat. Mater.* **2004**, *3*, 910-917.
99. Frattarelli, D.; Schiavo, M.; Facchetti, A.; Ratner, M.A.; Marks, T.J. Self-assembly from the gas-phase: Design and implementation of small-molecule chromophore precursors with large nonlinear optical responses. *J. Am. Chem. Soc.* **2009**, *131*, 12595-12612.
100. Kang, H.; Zhu, P.; Yang, Y.; Facchetti, A.; Marks, T.J. Self-assembled electrooptic thin films with remarkably blue-shifted optical absorption based on an X-shaped chromophore. *J. Am. Chem. Soc.* **2004**, *126*, 15974-15975.
101. Haller, M.; Liao, Y.; Plocinik, R.M.; Coffey, D.C.; Bhattacharjee, S.; Mazur, U.; Simpson, G.J.; Robinson, B.H.; Keller, S.L. Molecular self-assembly of mixed high-beta zwitterionic and neutral ground-state NLO chromophores. *Chem. Mater.* **2008**, *20*, 1778-1787.
102. Kwon, O.-P.; Ruiz, B.; Choubey, A.; Mutter, L.; Schneider, A.; Jazbinsek, M.; Gramlich, V.; Gunter, P. Organic nonlinear optical crystals based on configurationally locked polyene for melt growth. *Chem. Mater.* **2006**, *18*, 4049-4054.
103. Kwon, S.-J.; Hunziker, C.; Kwon, O.-P.; Jazbinsek, M.; Gunter, P. Large-area organic electro-optic single crystalline thin films grown by evaporation-induced local supersaturation with surface interactions. *Cryst. Growth Des.* **2009**, *9*, 2512-1516.
104. Kwon, S.-J.; Kwon, O.-P.; Jazbinsek, M.; Gramlich, V.; Gunter, P. Nonlinear optical co-crystal of analogous polyene chromophores with tailored physical properties. *Chem. Commun.* **2006**, *350*, 3729-3731.
105. Khan, R.U.A.; Kwon, O.-P.; Tapponnier, A.; Rashid, A.N.; Gunter, P. Supramolecular ordered organic thin films for nonlinear optical and optoelectronic applications. *Adv. Funct. Mater.* **2006**, *16*, 180-188.
106. Hunziker, C.; Kwon, S.-J.; Figi, H.; Juvalta, F.; Kwon, O.-P.; Jabinsek, M.; Gunter, P. Configurationally locked, phenolic polyene organic crystal 2-{3-(4-hydroxystyryl)-5,5-dimethylcyclohex-2-enylidene}malononitrile: Linear and nonlinear optical properties. *J. Opt. Soc. Am. B* **2008**, *25*, 1678-1683.
107. Figi, H.; Mutter, L.; Hunziker, C.; Jazbinsek, M.; Gunter, P.; Coe, B.J. Extremely large nonresonant second-order nonlinear optical response in crystals of the stilbazolium salt DAPSH. *J. Opt. Soc. Am. B* **2008**, *25*, 1786-1793.
108. Steier, W.H.; Chen, A.; Lee, S.-S.; Garner, S.M.; Zhang, H.; Ghuyanov, V.; Dalton, L.R.; Wang, F.; Ren, A.S.; Zhang, C.; *et al.* Polymer electro-optic devices for integrated optics. *Chem. Phys.* **1999**, *245*, 487-506.

109. Dalton, L.R. Nonlinear optical polymeric materials: From chromophore design to commercial applications. *Adv. Polym. Sci.* **2001**, *158*, 1-86.
110. Ma, H.; Jen, A.K.-Y.; Dalton, L.R. Polymer-based optical waveguide materials, processing, and devices. *Adv. Mater.* **2002**, *14*, 1339-1365.
111. Dalton, L.R. Rational design of organic electro-optic materials. *J. Phys.: Condens. Matter* **2003**, *15*, R897-R934.
112. Dalton, L.R. Organic Electro-Optic Materials. In *Handbook of Conducting Polymers*; Skotheim, T., Reynolds, J., Eds.; CRC Press/Marcel Dekker: Boca Raton, FL, USA, 2007; pp. 229-267.
113. Dalton, L.R.; Sullivan, P.; Bale, D.H.; Hammond, S.; Olbricht, B.C.; Rommel, H.; Eichinger, B.E.; Robinson, B.H. Organic Photonic Materials. In *Tutorials in Complex Photonic Media*; Noginov, M., McCall, M.W., Dewar, G., Zheludev, N.I., Eds.; SPIE Press: Bellingham, WA, USA, 2009; pp. 535-574.
114. Dalton, L.R.; Sullivan, P.A.; Bale, D.; Olbricht, B.; Davies, J.; Benight, S.; Kosilkin, I.; Robinson, B.H.; Eichinger, B.E.; Jen, A.K.-Y. Organic Electro-Optic Materials: Understanding Structure/Function Relationships Critical to the Optimization of Electro-Optic Activity. In *Organic Thin Films for Photonics Applications*; Herman, W., Foulger, S., Eds.; American Chemical Society: Washington, DC, USA, 2010; pp. 13-33.
115. Graf, H.M.; Zobel, O.; East, A.J.; Haarer, D. The polarized absorption spectroscopy as a novel method for determining the orientational order of poled nonlinear optical polymer films. *J. Appl. Phys.* **1994**, *75*, 3335-3340.
116. Mansuripur, M. Analysis of multilayer thin-film structures containing magneto-optic and anisotropic media at oblique incident using 2×2 matrices. *J. Appl. Phys.* **1990**, *67*, 6466-6476.
117. Steier, W.H.; Dalton, L.R. Polymer Modulators. In *Broadband Optical Modulators: Science, Technology, and Applications*; Chen, A., Murphy, E., Eds.; Taylor & Francis: New York, NY, USA, 2011; Chapter 9, pp. 221-254.
118. Kim, S.; Gleary, K.; Berini, P.; Dalton, L.R. Au and Ag nano-particle embedded plasmonic metal-slotted polymer electro-optic waveguide modulator. In *Proceedings of CLEO: Science and Innovations (CLEO: S and I)*, Baltimore, MD, USA, 1 May 2011; JWA69.